Published in final edited form as:
Biochem J. 2009 May 1; 419(3): 611–618. doi:10.1042/BJ20081888.

LIPID PHOSPHATE PHOSPHOHYDROLASE TYPE 1 (LPP1) DEGRADES EXTRACELLULAR LYSOPHOSPHATIDIC ACID *IN VIVO*

Jose L. Tomsig[*], **Ashley H. Snyder**[*], **Evgeny V. Berdyshev**[†], **Anastasia Skobeleva**[†], **Chifundo Mataya**[‡], **Viswanathan Natarajan**[†], **David N. Brindley**[‡], and **Kevin R. Lynch**[*]

[*] *Department of Pharmacology, University of Virginia, Charlottesville, Virginia 22908*

[†] *Department of Medicine, Biological Sciences Division, University of Chicago, Chicago, Illinois 60637*

[‡] *Department of Biochemistry, University of Alberta, Edmonton, T6G 2S2, Canada*

Abstract

Lysophosphatidic acid (LPA) is a lipid mediator that stimulates cell proliferation and growth and is involved in physiological and pathological processes such as wound healing, platelet activation, angiogenesis and the growth of tumors. Therefore, defining the mechanisms of LPA production and degradation are of interest in understanding the regulation of these processes. Extracellular LPA synthesis is relatively well understood whereas the mechanisms of its degradation are not. One route of LPA degradation is de-phosphorylation. A candidate enzyme is the integral membrane exophosphatase lipid phosphate phosphohydrolase type 1 (LPP1). We report here the development of a mouse wherein the LPP1 gene (*Ppap2a*) was disrupted. The homozygous mice, which are phenotypically unremarkable, generally lack LPP1 mRNA and multiple tissues exhibit a substantial (35–95%) reduction in LPA phosphatase activity. Compared to wild type littermates, $Ppap2a^{tr/tr}$ animals have increased levels of plasma LPA and LPA injected intravenously is metabolized at a four-fold slower rate. Our results demonstrate that LPA is rapidly metabolized in the bloodstream and that LPP1 is an important determinant of this turnover. These results indicate that LPP1 is a catabolic enzyme for LPA *in vivo*.

Keywords

LPA; LPP1; lipid phosphatase; LPA metabolism; PAP2a; exophosphatase

INTRODUCTION

Lysophosphatidic acid (LPA)[1] (1-acyl-2-lyso-*sn*-glycero-3-phosphate) has long been known as an intermediate in *de novo* biosynthesis of all glycerophospholipids. LPA gained credence as a signaling molecule with the discovery in the early 1990's by Moolenaar and collaborators that LPA promotes cell proliferation (see [1] for a review). LPA and other biologically active lipid phosphates, notably sphingosine 1-phosphate (S1P), have since been studied extensively and found to have a role as mediators in a variety of physiologic and pathologic processes. The stimulatory effect of LPA on cell proliferation, survival and migration serves as the underlying mechanism of the major biological effects of LPA. The most conspicuous examples are the

Address correspondence to: Kevin R. Lynch. Department of Pharmacology, University of Virginia, 1340 Jefferson Park Ave., Charlottesville, VA 22908. Tel.: 434-924-2840; Fax: 434-982-3878; E-mail: E-mail: krl2z@virginia.edu.

involvement of LPA in wound healing, platelet activation, vascular remodeling and the progression of some forms of cancer such as ovarian tumors (see [2] for a review).

The role of LPA and other lipid phosphates as first messengers was firmly established by the realization that many of the biological effects of these molecules are mediated by their interaction with specific, seven-transmembrane domain G protein-coupled receptors (see [3] for a review). As with any *bona fide* signaling molecule, specific mechanisms are expected to exist that ensure its timely destruction to prevent the detrimental effects of overstimulation. LPA catabolism is presumed to be mediated by a group of phosphatases termed lipid phosphate phosphohydrolases (LPPs) rather than phosphatidate phosphatase-1 (lipins) that are specific for phosphatidate [4,5].

LPPs (formerly known as phosphatidic acid phosphatases (PAPs) (see [6,7] for reviews) are enzymes that catalyze the hydrolysis of a variety of lipid phosphate mono-esters. The LPPs are Mg^{2+}-independent, NEM-insensitive (LPP1, LPP2 and LPP3 formerly known PAP2A, PAP2B and PAP2C respectively; see [8] for a review). LPP1-3 are cell surface, N-glycosylated, integral membrane proteins. LPP3 in some cell types also localizes to intracellular membranes [9]. The topology of membrane LPPs is such that the active site amino acids are exofacial, thus these enzymes function as exophosphatases [10].

The hypothesis that one or more LPP isotypes may function to delimit LPA signaling has been difficult to test. On the one hand, LPP1 and LPP3 are nearly ubiquitous among mammalian cells (see [11] for a review) and forced expression of these proteins is either toxic to cells or provide information restricted to cells in culture under somewhat artificial conditions [12,13]. On the other hand, the difficulties inherent in the study of integral membrane proteins – a lack of quality antibodies and purified protein – have slowed progress in understanding these enzymes. A chemical biology approach has not been particularly informative in that selective inhibitors have yet to be developed and structure activity relationship of substrates is rather uninformative. That is, the LPP isotypes act on a wide variety of lipid mono-phosphates including LPA, PA, diacylglycerolpyrophosphate, S1P and ceramide 1-phosphate. Using *in vitro* assays, LPP1 exhibits a preference for glycerol-versus sphingoid base-containing lipids, while LPP3 does not differentiate as well among these substrates (see [10] for a review). These ecto-activities of LPP1 have two potentially important functions. First, they could regulate circulating concentrations of LPA or S1P and thus the activation of their respective receptors. Decreased LPP activities occur in tumors and this has been proposed as a mechanism that results in increased LPA-induced growth in ovarian cancers [14]. Secondly, the dephosphorylated product formed by the LPP is taken up by the cell and thereby it stimulates cell signaling itself or after re-phosphorylation. [5,6,15,16].

An alternative approach – genetic manipulation – has yielded several studies reporting the consequences of altering the expression of LPP genes. Disruption of the mouse gene encoding LPP3 (*Ppap2b*) is embryonic lethal (E9.5), apparently as a consequence of aberrant embryonic and extra-embryonic development of the vasculature [17]. By contrast, mice lacking LPP2 (*Ppap2c* −/−) are viable, fertile and not noticeably different from wild type littermates [18]. Ablation of the *Drosophila* homologs of the mammalian LPPs (*wun* and *wun2*) results in a defect in germ cell migration, suggesting that a spatial pattern of phospholipid hydrolysis is required for the migration and survival of germ cells during fly development [19]. Global forced expression of LPP1 (*Ppap2a*) in mice resulted in runted animals with fur abnormalities and impaired spermatogenesis, a phenotype that is not readily ascribed to increased extracellular LPA or PA degradation. Interestingly, theses LPP1 transgenic mice had normal levels of plasma LPA [20].

In this communication we report the generation and characterization of a mouse strain wherein the gene encoding LPP1 (*Ppap2a*) is disrupted by insertion of an exon-trapping element. Mice with one ($Ppap2a^{+/tr}$) or both ($Ppap2a^{tr/tr}$) alleles disrupted are viable and fertile. We used these mice as an *in vivo* model to establish whether LPP1 plays a physiological role in controlling the degradation of circulating LPA. Our results demonstrate that LPP1 performs this function *in vivo*.

EXPERIMENTAL

Generation of LPP1 null mice

An embryonic stem (ES) cell line (RRD231) reported to harbor a gene trap vector (pGT1Lxf) in the first intron of the *Ppap2a* gene were obtained from BayGenomics via the Mutant Mouse Regional Resource Center (MMRRC) at Davis, CA. We verified the presence of the trapping element and further established its precise location by sequencing genomic DNA from $Ppap2a^{tr/tr}$ mice (see Fig. 1). Chimeric founder mice were generated at the University of Virginia Transgenic Mouse facility using C57BL/6 blastocysts. The ES cells were sv129 strain, animals used in this study were of mixed genetic background (F1N1, F1N5).

Genotyping of mice

Mice were genotyped by PCR using genomic DNA from tail biopsies, liver or brain samples and the following primers (see Fig. 1): 5′-GAGAGTGAGCGAGTGTCTGAGTTTCTGATG-3′ (forward), 5′-AGTACTGGGCATCTCACACCACAT-3′ (reverse wild type allele), 5′-CCTTCAAAGGGAAGGGGTAAAGTGGTAGGG-3′ (reverse trapped allele). Amplification in presence of 20 ng DNA and 4 mM $MgCl_2$ was carried out as follows: at 94 °C for 3 min, followed by 35 cycles at 94 °C (30 sec), 57 °C (1 min), 72 °C (1.5 min); and a final 72 °C step for 10 min.

Real-Time Reverse Transcriptase-Polymerase Chain Reaction (Real-Time RT-PCR)

RNA was extracted from tissues and cDNA was obtained using the SuperScript First-Strand Synthesis System (Invitrogen) using random hexamers according to the manufacturer's instructions. Amplification was performed in a iCycler iQ System (Bio-Rad, Hercules, CA) at 95 °C for 4 min, followed by 40 cycles at 95 °C, 55 °C, and 72 °C (30 s each step) in 50 μl of a SYBR Green-based medium (iQ SYBR Green Supermix; Bio-Rad) using the following forward and reverse primers: 5′-TGTACTGCATGCTGTTTGTCGCAC-3′, 5′-TGACGTCACTCCAGTGGTGTTTGT-3′ for LPP1; and 5′-ATAAACGATGCTGTGCTCTGTGCG-3′, 5-TTTGCTGTCTTCTCCTCTGCACCT-3′ for LPP3. The levels of mRNA expression were normalized to the expression level of the 18s ribosomal RNA gene measured using a commercial primer kit (QuantumRNA, Classic II; Ambion, Austin, TX). Quantitative gene expression was obtained from cycle differences at appropriate thresholds and the efficiency of amplification as described by Pfaffl [21]. The size and singularity of the RT-PCR products was established by agarose gel electrophoresis and melting point analysis. For the detection of the different LPP1 isoforms, a similar protocol was followed but using the following forward and reverse primers: 5′-ATCCATTTCAGAGGGGCTTT-3′, 5′-AACCTGCCCTCCTTGACTTT-3′ for isoform 1; and 5′-TTCAAGGCATACCCCCTTC-3′, 5′-GGTGGCTATGTAGGGATTGC-3′ for isoform 2. To amplify the cDNA region containing the trap insertion point in intron 2, a similar protocol was used except for annealing at 53 °C and the use of the following primer 5′-TCTGTTCCTCCCGCCACT-3′ in conjunction with the reverse primer used for LPP1 isoform 1.

[^{32}P]LPA and [^{32}P]PA synthesis

[^{32}P]-labeled LPA and PA were synthesized as previously described [22] using *E. coli* diacylglycerol kinase (Sigma D3065), ATP (Sigma A2383), γ-[^{32}P]ATP (MP Biochemicals 35001; 7,000 Ci/mmol), cardiolipin (Sigma C0563), and 1-monooleoyl-glycerol (Sigma M-7765) or 1,2-dioleoyl-glycerol (Avanti Polar Lipids 800811C). Final purification by thin layer chromatography (TLC) was carried out on Whatman Silica Gel plates (4865-621) using a mobile phase consisting of 1-butanol:acetic acid:H_2O 3:1:1. Small aliquots of the labeled compounds dissolved in chloroform were stored in light-protected, chloroform-rinsed glass vials at −20 °C for no more than four days. No radiolysis was observed under these conditions as judged by TLC analysis.

Measurement of lipid phosphate phosphohydrolase activity in tissue homogenates

Mice were anesthetized with isofluorane and sacrificed by cervical dislocation. Organs were immediately obtained, frozen in liquid nitrogen and stored at −80 °C. Brain samples consisted of tissue from the cerebral hemispheres. Skeletal muscle samples were obtained from the hind legs. Frozen tissue samples were homogenized using a motor driven Teflon pestle homogenizer in 10 volumes of 20 mM Tris-HCl, pH 7.5, 1 mM EGTA, 1 mM PMSF, 1mM DTT, 10 μg/ml aprotinin (Sigma A6279), 10 μg/ml leupeptin (Sigma L2023). Homogenates were centrifuged at 500 × g and the supernatant fluids were aliquoted and stored at −80 °C (pellets were discarded). The protein content of these preparations was measured according to Bradford [23] using a commercial Coomassie blue solution (Bio-Rad). LPP activity was measured as the release of [^{32}P]H_3PO_4 from [^{32}P]-labeled substrates presented as mixed Triton X-100 micelles as previously described [24] with some modifications. Assays were carried out in 200 μl of a buffer consisting of 20 mM Tris-HCl, pH 7.5, 1 mM MgCl2, 1 mM DTT, 3.2 mM Triton X-100, 100 μM LPA or PA and 50,000 dpm [^{32}P]LPA or [^{32}P]PA. Assays were carried out at 37 °C in presence of 100 μg protein for different times, 5 min to 30 min, according to the specific LPP activity of each tissue so that degradation did not exceed 5% of the total substrate. Different incubation times were preferred over incubation with different amounts of protein to preserve the ratio Triton X-100/protein content. Reactions were started by mixing 100 μl of mixed micelles with 100 μl of a solution containing the remaining components. Activity was constant with time for every tissue. No LPP activity was observed in absence of tissue. Reaction was stopped by adding 200 μl of 1 M $HClO_4$ containing 100 μM phosphoric acid. Samples were then centrifuged for 5 min at 15,000 × g and the supernatant extracted twice with H_2O-saturated 1-butanol. Orthophosphate was recovered from the extracted aqueous phase as described [25] by precipitation with 12.5 mM ammonium molybdate and extraction with isobutanol:benzene 1:1. Radionuclide in the organic phase was measured by liquid scintillation spectrometry. Specific activity of the substrates was determined by measuring the amount of ^{32}P present in known volumes of reaction media. To measure the NEM-sensitive, Mg^{2+}-independent activity, tissue samples containing 100 μg of protein were brought to 80 μl and supplemented with 10 μl of 50 mM NEM. After a 15 min incubation, NEM was neutralized by adding 10 μl of 22 mM DTT (1mM final DTT). This solution was then added to 100 μl of mixed micelles and processed as described above except for the omission of $MgCl_2$ and the addition of 1 mM EGTA and 2 mM EDTA [26].

Measurement the lipid phosphate phosphohydrolase activity of tissue slices and splenocytes

Ppap2a$^{+/+}$ and *Ppap2a*$^{tr/tr}$ mice were anesthetized with isofluorane and sacrificed by cervical dislocation. The brain hemispheres, kidney, liver and spleen were removed, placed in ice cold Buffer A (140 mM NaCl, 5 mM KCl, 1 mM $MgCl_2$, 5 mM glucose, 20 mM Hepes-NaOH, pH 7.4) and sliced into 300 μm thick slices using a Vibratome type slicer (Dosaka DTK 1500E microslicer). Slices were trimmed to approximately 3 mm × 3 mm squares and incubated in

200 μl of Buffer A containing 0.1% Fatty Acid Free bovine serum albumin (FAF-BSA, Sigma A6003), 100 μM LPA and approximately 2×10^5 cpm [^{32}P]LPA for variable times at 37 °C. At the end of the incubation periods, 100 μl aliquots were withdrawn and the presence of [^{32}P]H_3PO_4 was assayed as described for tissue homogenates. The remaining 100 μl were discarded and the tissue dissolved in 2% SDS and the protein content measured by the bicinchonic acid method using a commercial kit (Pierce 23223). Activity was linear with time. Linearity with protein concentration was tested only for slices of the same thickness and roughly the same size and shape. In particular, we carried out incubations with half, one or two 3 mm × 3 mm slices and found that activity and protein were linearly correlated. For slices of different thickness, activity and protein were not linearly correlated, therefore and to ensure thickness homogeneity similar organs from *Ppap2a*$^{+/+}$ and *Ppap2a*$^{tr/tr}$ were mounted together and sliced simultaneously. Splenocytes were obtained by passing the spleens through a nylon cell strainer (100 μm mesh, Falcon 352360) and discarding the capsule. Cells were resuspended in 1 ml of Buffer A and centrifuged at 300 × g for 5 min. The pellet was resuspended in 1 ml of erythrocyte lysis buffer (8.29 g/l NH_4Cl, 1 g/l $KHCO_3$, 0.0372 g/l Na_2EDTA, pH 7.3) and incubated on ice for 5 min. Lysis was quenched by adding 9 ml of Buffer A and washing the cell preparation twice (at 300 × g for 5 min each). Finally cells were resuspended cells in 1 ml Buffer A and counted in a hemocytometer. Viability, assessed by Trypan Blue exclusion, was > 99%. LPP activity was measured as described above and started by resuspending pellets (300 × g for 5 min) containing 5×10^5 lysed or non-lysed cells (approximately 100 and 20 μg of protein respectively) in 200 μl of reaction medium. In both cases, slices and splenocytes, incubation times were identical for similar tissues from *Ppap2a*$^{+/+}$ and *Ppap2a*$^{tr/tr}$ mice and they were adjusted for substrate degradation not to exceed 5%. No release of [^{32}P]H_3PO_4 was observed in absence of slices or cells.

Measurement of plasma LPA concentration

Plasma was obtained by cardiac puncture using EDTA (~ 5 mM) as anticoagulant. LPA levels were determined by liquid chromatography-tandem mass spectrometry using a hybrid ABI-4000 triple quadrupoleion trap mass spectrometer (Applied Biosystems, Foster City, CA) coupled with an Agilent 1100 liquid chromatography column and C17:0 LPA as an internal standard [27]. LPA species were separated on a Zorbax Eclipse XDB-C8 HPLC column (4.6 × 150 mm, 5 μm) using methanol/water/HCOOH, 79:20:0.5 v/v as solvent A and 99:0.5:0.5 v/v as solvent B, containing in both cases 5 mM NH_4COOH. Elution was carried out in solvent A for 1 min. A gradient change to solvent B lasting 1 min was then effected and a final, isocratic elution of LPA was carried out in solvent B for 7 min. LPA species were analyzed in negative ionization mode with declustering potential and collision energy optimized for 17:0, 18:0, 18:1, 18:2 and 20:4 LPA. Multiple reaction monitoring parameters for nine other LPA molecular species were selected with the closest possible approximation to the available LPA standards. The following transitions, indicated as the m/z values and, in parentheses, chain length: number of double bonds, were monitored: 407.0/153.0 (16:1); 409.0/153.1 (16:0); 423.0/153.1 (17:0, an unnatural species used as an internal standard); 431/153.0 (18:3); 433.0/153.0 (18:2); 435.1/152.9 (18:1); 437.0/153.0 (18:0); 455.1/153.0 (20:5); 457.0/153.0 (20:4); 459.1/153.0 (20:3); 461.1/153.0 (20:2); 481.1/153.0 (22:6); 483.1/153.0 (22:5); and 485.1/153.0 (22:4).

Preparation of plasma for clearance studies

A series of *Ppap2a*$^{+/+}$ and *Ppap2a*$^{tr/tr}$ mice were anesthetized and exsanguinated by cardiac puncture using EDTA (~5 mM) as anticoagulant. Plasma was prepared as previously described [28] by centrifuging the blood twice, at 1,000 and 10,000 × g for 3 min each time at 4 °C, and stored at −80 °C. Aliquots of these plasma preparations were used as a vehicle for [^{32}P]LPA to study LPA clearance as described below. Plasma used in clearance experiments was in each case of the same genotype as the animals whose clearance was being investigated.

Measurement of LPA clearance *in vitro*

Blood samples from a series of *Ppap2a*$^{+/+}$ and *Ppap2a*$^{tr/tr}$ mice were obtained and anticoagulated with EDTA (~ 5 mM). Half of these samples were used as whole blood and the other half used as plasma (obtained as described above). Blood and plasma samples were supplemented as soon as they were obtained with [^{32}P]LPA dissolved in either plasma (see above) or saline (0.9 % NaCl) containing 0.1% FAF-BSA. Incorporation of [^{32}P]LPA into plasma or saline solution was carried out by first drying in a glass vial an appropriate amount of [^{32}P]LPA dissolved in chloroform and then dissolving the dried [^{32}P]LPA into the appropriate vehicles (plasma or saline). Two hundred μl blood samples and 100 μl plasma samples were supplemented with plasma amounting to 5% of their volume (10 and 5 μl respectively) and containing approximately 10^5 cpm [^{32}P]LPA. Immediately after the addition of [^{32}P]LPA ("time zero" sample) or after 5, 15 and 30 min incubation at 37 °C, [^{32}P]LPA was measured as follows: plasma samples and plasma obtained from blood samples as described above were immediately acidified with 3.33 volumes of ice-cold 30 mM citric acid, 40 mM Na_2HPO_4, pH 4.0, and extracted twice with 8.88 volumes of H_2O-saturated butanol. Butanol extractions were then combined, dried under a stream of N_2, re-dissolved in chloroform and subjected to TLC as described above. Radioautographic analysis of the developed plates showed only one band that comigrates with authentic LPA (R_f = 0.5). LPA was then measured by scrapping off the LPA bands from the developed TLC plates and measuring their ^{32}P content by liquid scintillation spectrometry. The "time zero" plasma samples were also used to assess the quantitative recovery of LPA from plasma by comparing the amount of [^{32}P]LPA added to the plasma samples with the amount of [^{32}P]LPA recovered from TLC plates. Similar to the previously reported 99% recovery figure for this technique [29], our recovery was not significantly different from 100%.

Measurement of LPA clearance *in vivo*

Mice (24–27 g) were anesthetized with methoxyfluorane and injected through the tail vein with approximately 10^8 cpm [^{32}P]LPA (6.5×10^{-12} mole) dissolved in 150 μl of either plasma (see above) or sterile saline (0.9 % NaCl) containing 0.1% FAF-BSA. Immediately after injection, a blood sample (3 to 6 drops or approximately 50–100 μl) was taken by retro orbital bleeding using a Micro-Hematocrit capillary tube and EDTA (~5 mM) as anticoagulant. This first sample was obtained approximately 2–3 min after injection and it was considered to be the "time zero" sample. Additional samples were taken at 5 min, 15 min and 30 min. Immediately after they were obtained, blood samples were processed as described above to measure plasma [^{32}P]LPA. Similar to the *in vivo* experiments, no band other than LPA was observed by radioautography.

Measurement of LysoPLD activity

Plasma LysoPLD activity was measured according to Umezu-Goto *et al.* [30] by mixing 10 μl of plasma with 90 μl of a buffer consisting of 100 mM Tris-HCl, pH 9.0, 500 mM NaCl, 5 mM $MgCl_2$, 30 μM $CoCl_2$, 0.05% Triton X-100 and 1.1 mM LPC (Avanti Polar 148870). After 4 h incubation at 37 ° C, choline in samples was measured colorimetrically at 555 nm by adding 100 μl of 50 mM Tris-HCl, pH 8.0, 5 mM $MgCl_2$, 50 U/ml horseradish peroxidase, 18 U/ml choline oxidase, 5 mM 4-aminoantipyrine, and 3 mM N-ethyl-N-(2-hydroxy-3-sulfopropyl)-m-toluidine. Net production of choline was calculated by subtracting the amount of choline present in parallel samples that were kept frozen. Blood was obtained by retro-orbital bleeding using heparin as anticoagulant. Choline chloride (Fluka 26978) was used as standard.

Animal Care

The University of Virginia's Animal Care and Use Committee approved all experiments with animals.

RESULTS

Generation of *Ppap2a*$^{+/+}$ *Ppap2a*$^{+/tr}$ and *Ppap2a*$^{tr/tr}$ mice

We first established the exact location of the exon trap element by sequencing genomic DNA from *Ppap2a*$^{tr/tr}$ mice. As shown in Fig. 1A, insertion occurred in intron 1 as reported by BayGenomics. Mouse LPP1 is expressed as two different isoforms as a result of alternative splicing of exon 2 [31]. However, in the present instance, both variants were expected to be trapped because insertion occurred upstream of either exon 2 (Fig. 1A). Based on the location of the trap element we designed primers to detect by PCR the normal and trapped versions of the gene and were able to identify wild type, heterozygous and homozygous animals or *Ppap2a*$^{+/+}$, *Ppap2a*$^{+/tr}$ and *Ppap2a*$^{tr/tr}$ animals (Fig. 1B).

Ppap2a$^{tr/tr}$ and *Ppap2a*$^{+/tr}$ mice are phenotypically unremarkable, that is their anatomy, behavior, and fertility are not readily distinguished from those of wild type littermates. We examined the gross anatomy of all major organs of these animals and found no differences with wild type animals. Our examination included the male reproductive tract and the prostate in particular because LPP1 mRNA is particularly prominent in prostate and LPP1 is an androgen-induced gene [32].

LPP1 mRNA expression

We investigated next the levels of LPP1 mRNA expression in different organs of *Ppap2a*$^{tr/tr}$ and *Ppap2a*$^{+/+}$ mice by quantitative Real-Time RT-PCR. In these experiments, primers were anchored to exons 3 and 4 (forward primer) and 5 (reverse primer) and therefore results correspond to the combined expression of both LPP1 isoforms which, as depicted in Fig. 1A, are generated by alternative splicing of exon 2. As presented in Fig. 2, *Ppap2a*$^{tr/tr}$ mice exhibited much reduced levels of LPP1 expression in relation to *Ppap2a*$^{+/+}$ littermates in all organs studied except the brain. LPP1 mRNA expression in *Ppap2a*$^{tr/tr}$ mice ranged from 1/300 (kidney) to 1/800 (muscle) the levels found in *Ppap2a*$^{+/+}$ mice. The unaltered expression of LPP1 mRNA in the brain prompted us to investigate whether these animals lack the trapping element in this organ, but we found no evidence for a wild type allele in *Ppap2a*$^{tr/tr}$ mice in brain genomic DNA (not shown). Further, we found no difference in the expression of LPP1 mRNA isoforms in comparing brains of *Ppap2a*$^{tr/tr}$ and *Ppap2a*$^{+/+}$ mice (not shown). Finally, we examined the expression of LPP3 in the same organs and found that, unlike LPP1, levels of LPP3 expression in *Ppap2a*$^{tr/tr}$ and *Ppap2a*$^{+/+}$ mice were similar (Fig. 2).

LPA phosphatase activity

Tissue homogenates from *Ppap2a*$^{tr/tr}$ mice exhibited reduced phosphatase activity in all organs studied except the brain, although that the extent of reduction varied among tissues (Fig. 3A). Using [^{32}P]LPA as a substrate, we observed values ranging from 43% in heart (*i.e.* activity in *Ppap2a*$^{tr/tr}$ mice was 57% that of *Ppap2a*$^{+/+}$ mice) to 91% in the spleen. With [^{32}P]PA as a substrate, values ranged from 31% in the kidney to 88% in the spleen. We found major differences in LPP activity between the brain and the other organs studied. As predicted from LPP1 mRNA quantification, LPA phosphohydrolase activity was not diminished in brain tissue from *Ppap2a*$^{tr/tr}$ mice. We also found that the lipid phosphohydrolase activity from both *Ppap2a*$^{tr/tr}$ and *Ppap2a*$^{+/+}$ mice was higher with PA (vs. LPA) as a substrate in brain homogenates as compared to other tissues. *In toto*, these results lead us to conclude that *Ppap2a*$^{tr/tr}$ mice are not entirely null for LPP1, rather these animals are LPP1 hypomorphs that exhibit severely reduced expression of LPP1 mRNA and reduced LPP activity in all organs studied except the brain.

As mentioned in the Introduction, LPPs such as LPP1 are NEM-insensitive, Mg^{2+}-independent and act as exophosphatases, *i.e.* degrade lipids presented to the extracellular face of the cell

membrane. A second group of lipid phosphohydrolases have opposite characteristics: they are sensitive to NEM, require Mg^{2+} and are located inside the cells. We carried out a series of experiments to further map to LPP1 the reduction of lipid phosphohydrolase activity observed in *Ppap2a*$^{tr/tr}$ mice. To this end, we investigated first the effects of NEM alkylation and lack of Mg^{2+} on our assay of tissue phosphohydrolase activity (Fig. 3A), and, second, the exophosphatase activity of intact tissues (Fig. 4). As shown in Fig. 3A, only a small fraction of the total activity was NEM-sensitive. We compared the NEM-sensitive, Mg^{2+}-dependent fractions from similar organs of *Ppap2a*$^{tr/tr}$ and *Ppap2a*$^{+/+}$ mice and found that in some cases *Ppap2a*$^{tr/tr}$ mice show an increased amount of NEM-sensitive, Mg^{2+}-dependent activity. This phenomenon is illustrated in Fig. 3B, where the *Ppap2a*$^{tr/tr}$/*Ppap2a*$^{+/+}$ ratio of NEM-sensitive, Mg^{2+}-dependent activities is shown for each organ. In the cases of the kidney, liver and muscle, ratios were much higher than unity: 7.6, 5.9 and 15 respectively. For the other organs studied, values ranged from 0.83 to 1.1.

LPA exophosphatase activity

The topology of LPP1 is such that the active site is at the cell surface, thus we measured exophosphatase activity (Fig. 4). We prepared tissue slices from different organs, incubated them with [^{32}P]LPA and measured the release of [^{32}P]H_3PO_4. Similar to our previous findings with tissue homogenates, *Ppap2a*$^{tr/tr}$ mice organs, with the exception of the brain, showed a decreased level of exophosphatase activity and, once again, the spleen was the most severely affected organ. Values were 65, 74 and 94 % reduction for the kidney, liver and spleen (Figs. 2 and 3). We examined in more detail the exophosphatase activity of the spleen. Splenocytes isolated from *Ppap2a*$^{tr/tr}$ mice exhibit, as expected, a greatly reduced exophosphatase activity (> 99%)

Plasma LPA levels

If LPP1 metabolizes LPA *in vivo*, the reduced levels of LPA phosphohydrolase activity in *Ppap2a*$^{tr/tr}$ mice should result in elevated levels of plasma LPA. We tested this prediction by measuring plasma LPA levels in *Ppap2a*$^{tr/tr}$ and *Ppap2a*$^{+/+}$ mice by LC-MS-MS. We found that *Ppap2a*$^{tr/tr}$ mice have higher levels of plasma LPA on average, but there was substantial variation in LPA levels among animals (Fig 5). To determine the source of this variation, we measured plasma LPA levels in a homogeneous population of pure C57BL/6j mice. We found that LPA levels in age- and gender-matched C57BL/6j mice were in agreement with previously reported values (see Discussion) and exhibited low variability (Fig. 5). This result suggests that the observed difference in plasma LPA levels between *Ppap2a*$^{tr/tr}$ and *Ppap2a*$^{+/+}$ mice is genuine and the wide range of LPA plasma values is a reflection of a diverse (genetically as well as age and gender) population. To test this idea, we backcrossed the mutant *Ppap2a* mice against C57BL/6j mice for four additional generations. After ascertaining that mutant and wild type the F1N5 mice retained the differences in LPP1 mRNA and activity delineated above, we measured plasma LPA levels. Although the F1N5 mice had much less variation in plasma LPA levels, the difference between *Ppap2a*$^{tr/tr}$ mice and their wild type littermates remained (Fig. 5). Interestingly, the mole fractions of the LPA species measured was not different in *Ppap2a*$^{tr/tr}$ and *Ppap2a*$^{+/+}$ mice (not shown). The rank order of abundance was as follows: 18:2 > 20:4 > 22:6 > 18:0 ~ 16:0 > 18:1 > 20:3 ~ 22:5 > 16:1 ~ 22:4 ≫14:0 ~ 20:5 ~ 20:2 ≫ 22:3 ~ 22:2. This result suggests that LPP1 is not selective for any of these molecular species.

Degradation of LPA in blood

Next we examined the ability of *Ppap2a*$^{tr/tr}$ and *Ppap2a*$^{+/+}$ mice to metabolize LPA by measuring the rate of disappearance of [^{32}P]LPA in blood both *ex vivo* and *in vivo*. Fig. 6A documents that the amount of LPA that can be recovered from whole blood incubated at 37° C rapidly diminished as a function of time. The rate of decay was slower for blood obtained

from *Ppap2a*$^{tr/tr}$ mice. Half-lives were approximately 5 and 20 min for *Ppap2a*$^{+/+}$ and *Ppap2a*$^{tr/tr}$ mice, respectively. Similar experiments measuring the decay in plasma samples revealed that [^{32}P]LPA was stable in plasma up to 30 min (not shown). Fig. 6B shows a similar series of experiments except that in this case [^{32}P]LPA was injected into the bloodstream of mice. In this case decay was faster and, similar to the *ex vivo* observations, disappearance of [^{32}P]LPA was markedly slower in *Ppap2a*$^{tr/tr}$ mice. Half lives in this case were approximately 3 and 12 min. Fig. 6 also documents that there were no differences in [^{32}P]LPA decay when a less physiologic alternative — saline solution containing FA-free BSA — was used as a vehicle for [^{32}P]LPA instead of plasma. Finally, we explored whether *Ppap2a*$^{tr/tr}$ animals show any abnormality in the production of LPA, likely a compensatory reduction as a consequence of the elevated plasma LPA levels and the reduced rate of LPA degradation. We found no differences between *Ppap2a*$^{+/+}$ and *Ppap2a*$^{tr/tr}$ mice when we used a colorimetric method to detect choline produced by the breakdown of LPC into choline and LPA catalyzed by plasma lysophospholipase D. Values were (average ± S.D. of 5 animals): 7.53 ± 0.21 and 7.73 ± 0.23 × 10^{-13} moles choline/μl plasma/min.

DISCUSSION

In vitro studies have implicated LPP1 in the phosphohydrolysis of extracellular LPA, but the lack of specific inhibitors has made testing the physiologic relevance of LPP1 in this process difficult. With this paper we document that disruption of the LPP1 encoding gene, *Ppap2a*, results in mice with substantially reduced NEM-resistant LPA/PA phosphatase activity, moderately elevated plasma LPA levels and slowed clearance of exogenously administered LPA. Our data demonstrate that LPP1 contributes 43–81% of the total tissue LPA phosphohydrolase activity and 65–99% of the exophosphatase activity. We suppose that the residual LPA/PA phosphatase activity is due to other lipid phosphatases such as LPP3. Our results support the contention LPP1 is a physiologically relevant LPA exophosphatase.

Exophosphatase activity was virtually nil in *Ppap2a*$^{tr/tr}$ splenocytes suggesting that LPP1 is the only functioning exo-LPP in these cells. This is a somewhat surprising observation in view of the presence of LPP3 mRNA in splenocytes. Nevertheless, the lack of LPA exophosphatase activity may be exploited to examine the role of LPP1 further.

The unaltered level of LPP1 mRNA expression and enzyme activity in the brains of *Ppap2a*$^{tr/tr}$ mice was unexpected. The possibility that *Ppap2a*$^{tr/tr}$ mice lack the trapping element in brain tissue, *i.e.* mosaicism, was ruled out by genotyping brain DNA. We reasoned that alternative splicing might be responsible for the failure of the exon trapping element in brain but we were unable to detect differential expression of known LPP1 isoforms [31]. Thus we do not have a plausible explanation as to why the pre-mRNA splicing machinery does not recognize the exon trap splicing acceptor site in brain.

Our LPP1 hypomorphic mice have elevated plasma LPA levels. The range of reported mouse plasma LPA concentrations is 170–625 nM [34,35,36,37]. The lowest concentration detected in our LPP1 mice was 368 nM, while the highest was 2.45 μM (Fig. 5). We considered whether the source this large variation in LPA levels was an artifact of our methods (plasma preparation, LC-MS-MS) or a reflection of the genetic diversity of our LPP1 colony (F1N1, C57BL/6 x sv129 strains). When one of our laboratories (KRL) generated plasma from age- and gender-matched pure-bred C57BL/6j mice and blinded another of our laboratories (VN) to the source of this plasma, our methods yielded values that were similar to previously reported mouse plasma LPA concentrations and, most importantly, exhibited much less variation: 348 ± 98 nM, *i.e.* 28%. Additionally, the intra-assay variability was found to be slight (Fig. 5). Thus we reasoned that the disparity in plasma LPA levels measured in our F1N1 *Ppap2a*$^{tr/tr}$ mice was due largely to differences in genetic background and, perhaps, in gender and age. When our

LPP1 mouse colony was re-derived at F1N5 after additional crossings onto the C57Bl/6j background, the variability in plasma LPA levels was substantially reduced in age-matched mice (Fig. 5). Nonetheless, our data indicate consistently that LPP1-deficient mice exhibit plasma LPA levels significantly higher than control littermates supporting the hypothesis that LPP1 acts as an LPA exophosphatase. Further, our results document that plasma LPA levels can exceed 2 μM in mice without apparent ill-effects.

We also investigated the ability of *Ppap2a*$^{tr/tr}$ mice to catabolize LPA by comparing the rate of disappearance of tracer amounts of [^{32}P]LPA from the blood of *Ppap2a*$^{tr/tr}$ and *Ppap2a*$^{+/+}$ animals. We found that [^{32}P]LPA disappears rapidly from the blood of *Ppap2a*$^{+/+}$ animals when incubated *ex vivo* at 37 °C and that this process is even faster *in vivo*. As Fig. 6 documents, *Ppap2a*$^{tr/tr}$ mice exhibit, both *ex vivo* and *in vivo*, a still rapid but distinctly slower rate of LPA disappearance. We have measured only how much LPA remains after injection so it is not possible to ascribe the disappearance of exogenous LPA to any catabolic process. Nevertheless, the mutant mice demonstrate that LPP1 is in part responsible for this process.

In conclusion, we developed an LPP1 hypomorph mouse that enabled us to provide a definitive demonstration that LPP1 plays a role in the extracellular catabolism of LPA in intact animals under physiological circumstances. Further, our results suggest a role of LPP1 in controlling the kinetics of extracellular LPA turnover *in vivo*. These results provide evidence that LPP1 is an important determinant of LPA turnover and circulating LPA concentrations, which might alter LPA signaling patterns.

Acknowledgements

The authors thank Dr. Timothy Bender, Department of Microbiology, University of Virginia, for assisting us with the preparation of splenocytes, as well as Gina Wimer and Perry C. Kennedy for their help with mouse manipulations. This work was supported by National Institute of Health grants R01 GM052722 (to K.R.L.), R01 HL079396 (to V.N.), T32 GM007055 (to A.H.S.) and by the Canadian Institutes of Health Research MOP 81137 (to D.N.B.).

Abbreviations used

LPA
lysophosphatidic acid

S1P
sphingosine 1-phosphate

LPP
lipid phosphate phosphohydrolase

PAP
phosphatidic acid phosphatase

RT-PCR
Reverse Transcriptase-Polymerase Chain Reaction

PA
phosphatidic acid

NEM
N-ethylmaleimide

TLC
thin layer chromatography

LPC

lysophosphatidyl-choline

PCR

polymerase chain reaction

FAF-BSA

fatty acid-free bovine serum albumin

References

1. Moolenaar WH. Development of our current understanding of bioactive lysophospholipids. Annals NY Acad Sci 2000;905:1–10.
2. van Meeteren LA, Moolenaar WH. Regulation and biological activities of the autotaxin-LPA axis. Prog Lipid Res 2007;46:145–160. [PubMed: 17459484]
3. Anliker B, Chun J. Regulation and biological activities of the autotaxin-LPA axis. J Biol Chem 2004;279:20555–20558. [PubMed: 15023998]
4. Reue K, Brindley DN. Multiple roles for lipins/phosphatidate phosphatase enzymes in lipid metabolism. J Lipid Res 2008;49:2493–503. [PubMed: 18791037]
5. Brindley DN, Pilquil C. Lipid phosphate phosphatases and signaling. J Lipid Res. 200810.1194/jlr.R800055-JLR200Epub ahead of print
6. Brindley DN. Lipid phosphate phosphatases and related proteins: signaling functions in development, cell division, and cancer. J Cell Biochem 2004;92:900–912. [PubMed: 15258914]
7. Pyne S, Long JS, Ktistakis NT, Pyne NJ. Lipid phosphate phosphatases and lipid phosphate signaling. Biochem Soc Trans 2005;33:1370–1374. [PubMed: 16246121]
8. Carman GM, Han GS. Roles of phosphatidate phosphatase enzymes in lipid metabolism. Trends Biol Sci 2006;31:694–699.
9. Sciorra VA, Morris AJ. Sequential actions of phospholipase D and phosphatidic acid phosphohydrolase 2b generate diglyceride in mammalian cells. Mol Biol Cell 1999;10:3863–3876. [PubMed: 10564277]
10. Zhang QX, Pilquil CS, Dewald J, Berthiaume LG, Brindley DN. Identification of structurally important domains of lipid phosphate phosphatase-1: implications for its sites of action. Biochem J 2000;345:181–184. [PubMed: 10620492]
11. Pyne S, Kong KC, Darroch PI. Lysophosphatidic acid and sphingosine 1-phosphate biology: the role of lipid phosphate phosphatases. Semin Cell Dev Biol 2004;15:491–501. [PubMed: 15271294]
12. Alderton F, Darroch P, Sambi B, McKie A, Ahmed IS, Pyne N, Pyne S. G-protein-coupled receptor stimulation of the p42/p44 mitogen-activated protein kinase pathway is attenuated by lipid phosphate phosphatases 1, 1a, and 2 in human embryonic kidney 293 cells. J Biol Chem 2001;276:13452–13460. [PubMed: 11278307]
13. Pilquil C, Dewald J, Cherney A, Gorshkova I, Tigyi G, English D, Natarajan V, Brindley DN. Lipid phosphate phosphatase-1 regulates lysophosphatidate-induced fibroblast migration by controlling phospholipase D2-dependent phosphatidate generation. J Biol Chem 2006;281:33418–33429.
14. Tanyi JL, Hasegawa Y, Lapushin R, Morris AJ, Wolf JK, Berchuck A, Lu K, Smith DI, Kalli K, Hartmann LC, McCune K, Fishman D, Broaddus R, Cheng KW, Atkinson EN, Yamal JM, Bast RC, Felix EA, Newman RA, Mills GB. Role of decreased levels of lipid phosphate phosphatase-1 in accumulation of lysophosphatidic acid in ovarian cancer. Clin Cancer Res 2003;9:3534–3545. [PubMed: 14506139]
15. Sigal YJ, McDermott MI, Morris AJ. Integral membrane lipid phosphatases/phosphotransferases: common structure and diverse functions. Biochem J 2005;387:281–293. [PubMed: 15801912]
16. Zhao Y, Kalari SK, Usatyuk PV, Gorshkova I, He D, Watkins T, Brindley DN, Sun C, Bittman R, Garcia JG, Berdyshev EV, Natarajan V. Intracellular generation of sphingosine 1-phosphate in human lung endothelial cells: role of lipid phosphate phosphatase-1 and sphingosine kinase 1. J Biol Chem 2007;282:14165–14177. [PubMed: 17379599]

17. Escalante-Alcalde D, Hernandez L, Le Stunff H, Maeda R, Lee HS, Gang-Cheng J, Sciorra VA, Daar I, Spiegel S, Morris AJ, Stewart CL. The lipid phosphatase LPP3 regulates extra-embryonic vasculogenesis and axis patterning. Development 2003;130:4623–4637. [PubMed: 12925589]
18. Zhang N, Sundberg JP, Gridley T. Mice mutant for Ppap2c, a homolog of the germ cell migration regulator wunen, are viable and fertile. Genesis 2000;27:137–140. [PubMed: 10992322]
19. Starz-Gaiano M, Cho NK, Forbes A, Lehmann R. Spatially restricted activity of a Drosophila lipid phosphatase guides migrating germ cells. Development 2001;128:983–991. [PubMed: 11222152]
20. Yue J, Yokoyama K, Balazs L, Baker DL, Smalley D, Pilquil C, Brindley DN, Tigyi G. Mice with transgenic overexpression of lipid phosphate phosphatase-1 display multiple organotypic deficits without alteration in circulating lysophosphatidate level. Cell Signal 2004;16:385–399. [PubMed: 14687668]
21. Pfaffl MW. A new mathematical model for relative quantification in real-time RT-PCR. Nucleic Acids Res 2001;29:2002–2007.
22. Han GS, Carman GM. Assaying lipid phosphate phosphatase activities. Methods Mol Biol 2004;284:209–216. [PubMed: 15173618]
23. Bradford MM. A rapid and sensitive method for the quantitation of microgram quantities of protein utilizing the principle of protein-dye binding. Anal Biochem 1976;72:248–254. [PubMed: 942051]
24. McDermott MI, Sigal YJ, Crump JS, Morris AJ. Enzymatic analysis of lipid phosphate phosphatases. Methods 2006;39:169–179. [PubMed: 16815033]
25. Jasinska R, Zhang QX, Pilquil C, Singh I, Xu J, Dewald J, Dillon DA, Berthiaume LG, Carman GM, Waggoner DW, Brindley DN. Lipid phosphate phosphohydrolase-1 degrades exogenous glycerolipid and sphingolipid phosphate esters. Biochem J 1999;340:677–686. [PubMed: 10359651]
26. Han GS, Siniossoglou S, Carman GM. The cellular functions of the yeast lipin homolog PAH1p are dependent on its phosphatidate phosphatase activity. J Biol Chem 2007;282:37026–37035. [PubMed: 17971454]
27. Georas SN, Berdyshev E, Hubbard W, Gorshkova IA, Usatyuk PV, Saatian B, Myers AC, Williams MA, Xiao HQ, Liu M, Natarajan V. Lysophosphatidic acid is detectable in human bronchoalveolar lavage fluids at baseline and increased after segmental allergen challenge. Clin Exp Allergy 2007;37:311–322. [PubMed: 17359381]
28. Baker DL, Morrison P, Miller B, Tolley B, Westermann AM, Bonfrer JMG, Moolenaar WH, Tigyi GJ. Plasma lysophosphatidic acid concentration and ovarian cancer. J Amer Med Assoc 2002;287:3081–3082.
29. Baker DL, Desiderio DM, Miller DD, Tolley B, Tigyi GJ. Direct quantitative analysis of lysophosphatidic acid molecular species by stable isotope dilution electrospray ionization liquid chromatography-mass spectrometry. Anal Biochem 2001;292:287–295. [PubMed: 11355863]
30. Umezu-Goto M, Kishi Y, Taira A, Hama K, Dohmae N, Takio K, Yamori T, Mills GB, Inoue K, Aoki J, Arai H. Autotaxin has lysophospholipase D activity leading to tumor cell growth and motility by lysophosphatidic acid production. J Cell Biol 2002;158:227–233. [PubMed: 12119361]
31. Leung DW, Tompkins CK, White T. Molecular cloning of two alternatively spliced forms of human phosphatidic acid phosphatase cDNAs are differentially expressed in normal and tumor cells. DNA Cell Biol 1998;17:377–385. [PubMed: 9570154]
32. Ulrix W, Swinnen JV, Heyns W, Verhoeven G. Identification of the phosphatidic acid phosphatase type 2a isozyme as an androgen-regulated gene in the human prostatic adenocarcinoma cell line LNCaP. J Biol Chem 1998;273:4660–4665. [PubMed: 9468526]
33. Kai M, Sakane F, Jia YJ, Imai S, Yasuda S, Kanoh H. Lipid phosphate phosphatases 1 and 3 are localized in distinct lipid rafts. J Biochem 2006;140:677–686. [PubMed: 17005594]
34. Saulnier-Blache JS, Girard A, Simon MF, Lafontan M, Valet P. A simple and highly sensitive radioenzymatic assay for lysophosphatidic acid quantification. J Lipid Res 2000;41:1947–1951. [PubMed: 11108727]
35. Tanaka M, Okudaira S, Kishi Y, Ohkawa R, Iseki S, Ota M, Noji S, Yatomi Y, Aoki J, Arai H. Autotaxin stabilizes blood vessels and is required for embryonic vasculature by producing lysophosphatidic acid. J Biol Chem 2006;281:25822–25830. [PubMed: 16829511]
36. van Meeteren LA, Ruurs P, Stortelers C, Bouwman P, von Rooijen MA, Pradère JP, Pettit TR, Wakelam MJO, Saulnier-Blache JS, Mummery CL, Moolenaar WH, Jonkers J. Autotaxin, a secreted

lysophospholipase D, is essential for blood vessel formation during development. Mol Cell Biol 2006;26:5015–5022. [PubMed: 16782887]

37. Pamuklar Z, Federico L, Liu S, Umezu-Goto M, Dong A, Panchatcharam M, Fulerson Z, Berdyshev W, Natarajan V, Fang F, van Meeteren LA, Moolenaar WH, Mills GB, Morris AJ, Smith SS. Autotaxin/lysophospholipase D and lysophosphatidic acid regulate murine hemostasis and thrombosis. J Biol Chem. 200910.1074/jbc.M807820200Epub ahead of print

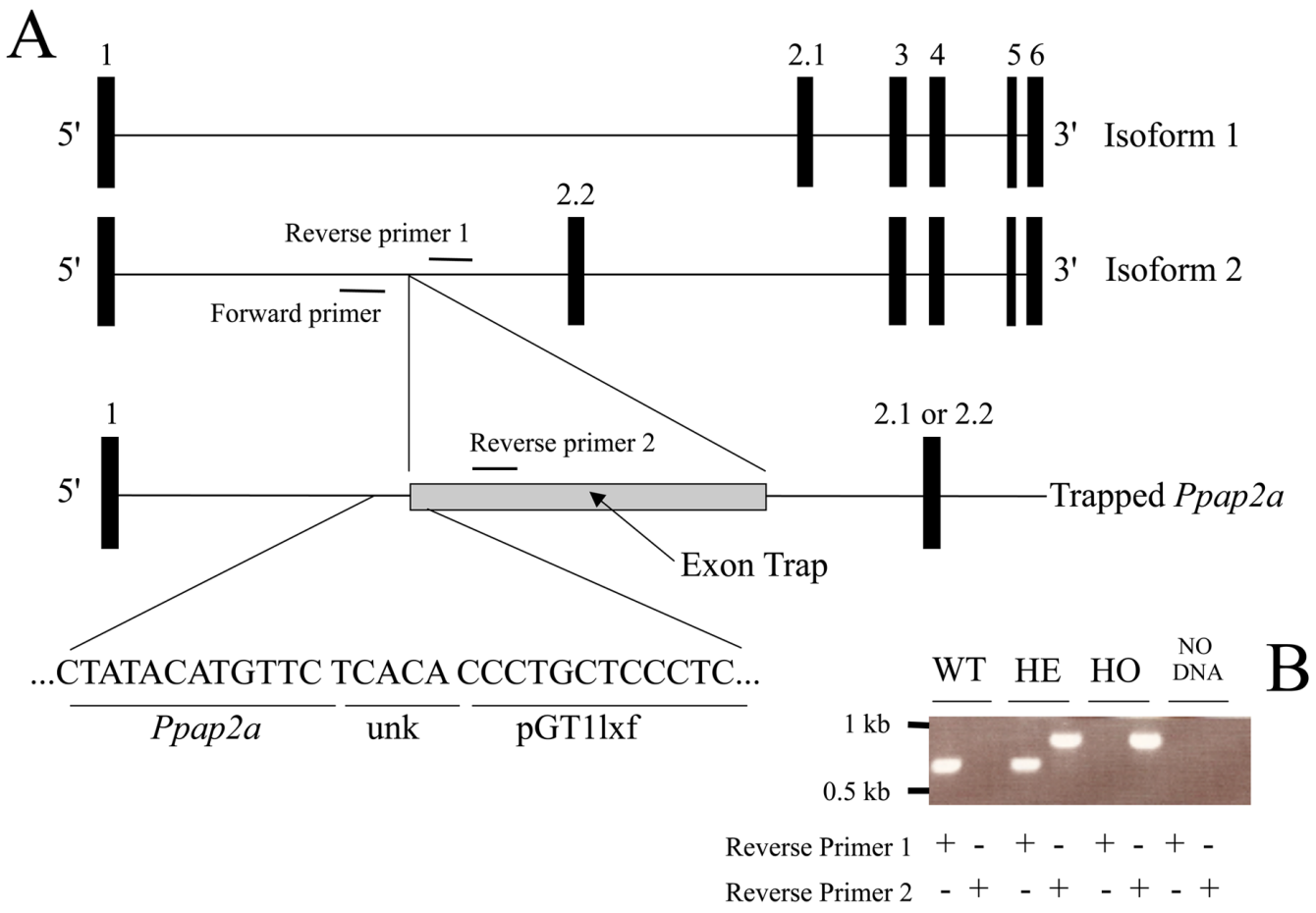

FIGURE 1. Structure and characterization of the normal and trapped *Ppap2a* mouse genes

A schematic representation of the normal and trapped *Ppap2a* alleles are shown in A. The wild type *Ppap2a* gene consist of six exons (numbered 1 to 6 in figure) located on chromosome 13. Two isoforms arise by alternative splicing of two different exons 2 (2.1 and 2.2). Mice used in this study harbor an exon trapping element ("Exon Trap" in figure) between exons 1 and 2 and therefore generate a truncated mRNA ("Trapped *Ppap2a*" in figure) consisting of exon 1 spliced to the coding sequence of the trapping element followed by a poly(A) sequence. Because insertion occurred upstream of exons 2, only one trapped isoform exists. The exact location of the trapping element was determined by genomic DNA sequencing and found to be some 25,600 bp downstream of the 5′ end of the gene (about 75% the length of intron 1). Sequence at the insertion point shows an intervening 5-nucleotide sequence of unknown origin ("unk") between the *Ppap2a* gene and the trap element sequence ("pGT1Lxf"). Genotyping was carried out by PCR amplification of genomic DNA using a forward primer complementary to a sequence upstream of the insertion point, and two reverse primers corresponding to sequences downstream in the normal and in the trapped gene. Expected products sizes were 675 bp and 931 bp for the normal and trapped genes respectively. The analysis of PCR products by agarose gel electrophoresis for homozygous ($Ppap2a^{tr/tr}$, "HO" in figure), heterozygous ($Ppap2a^{+/tr}$,"HE" in figure) and wild type ($Ppap2a^{+/+}$, "WT" in figure) animals using the indicated combinations of forward and reverse primers is shown in B. In A, the relative positions of the exons and the trap element are shown according to their actual locations within the gene, exon sizes however have been exaggerated for clarity (they constitute only about 2% of the gene).

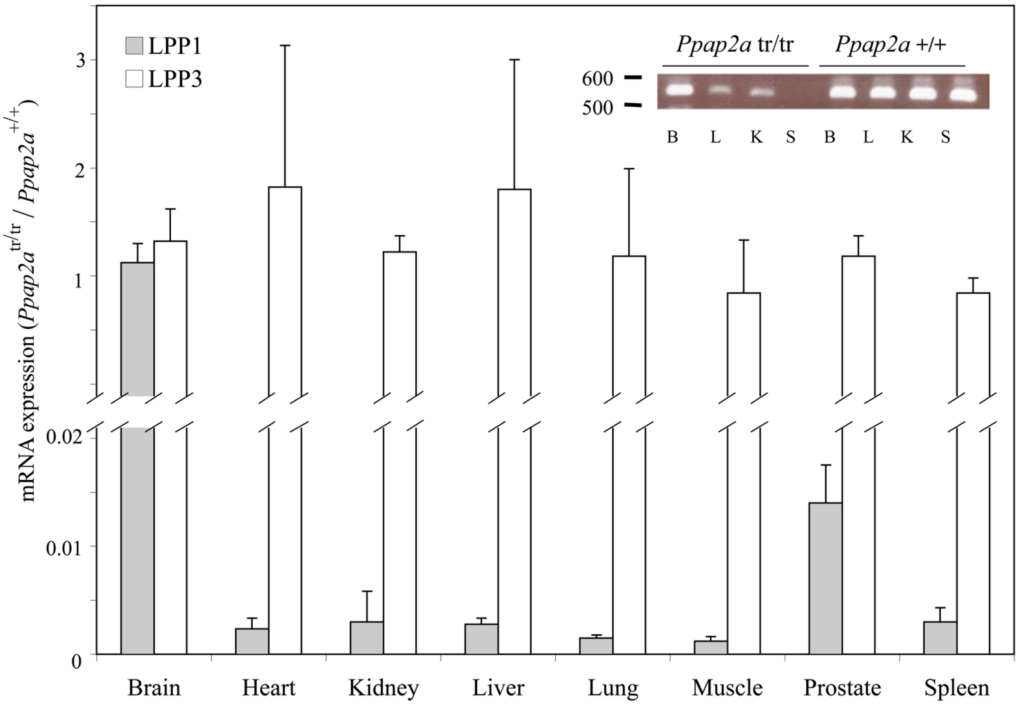

FIGURE 2. LPP1 and LPP3 mRNA expression in selected organs of *Ppap2a*$^{tr/tr}$ and *Ppap2a*$^{+/+}$ mice

The expression of LPP1 and LPP3 mRNA was measured by Real-Time RT-PCR in *Ppap2a*$^{tr/tr}$ and *Ppap2a*$^{+/+}$ mice. In the case of LPP1, appropriate primers were used to obtain the combined expression of both isoforms (see Results). mRNA expression for LPP1 and LPP3 was normalized by the expression of the 18s ribosomal RNA gene. The main figure shows the expression of mRNA for LPP1 (gray bars) and LPP3 (white bars) as a ratio (*Ppap2a*$^{tr/tr}$/ *Ppap2a*$^{+/+}$). Data correspond to the average ± S.D. of three ratios measured in three different pairs of animals (Note the split y axis). Inset (top right) shows the expression of LPP1 mRNA in the brain, liver, kidney and spleen ("B", "L", "K" and "S" in figure) of *Ppap2a*$^{tr/tr}$ and *Ppap2a*$^{+/+}$ mice. In this case a standard PCR reaction was carried out for 33 cycles using a forward primer anchored to exon 1 and a reverse primer anchored to exons 3 and 4. The expected molecular mass of the PCR product is 531 bp.

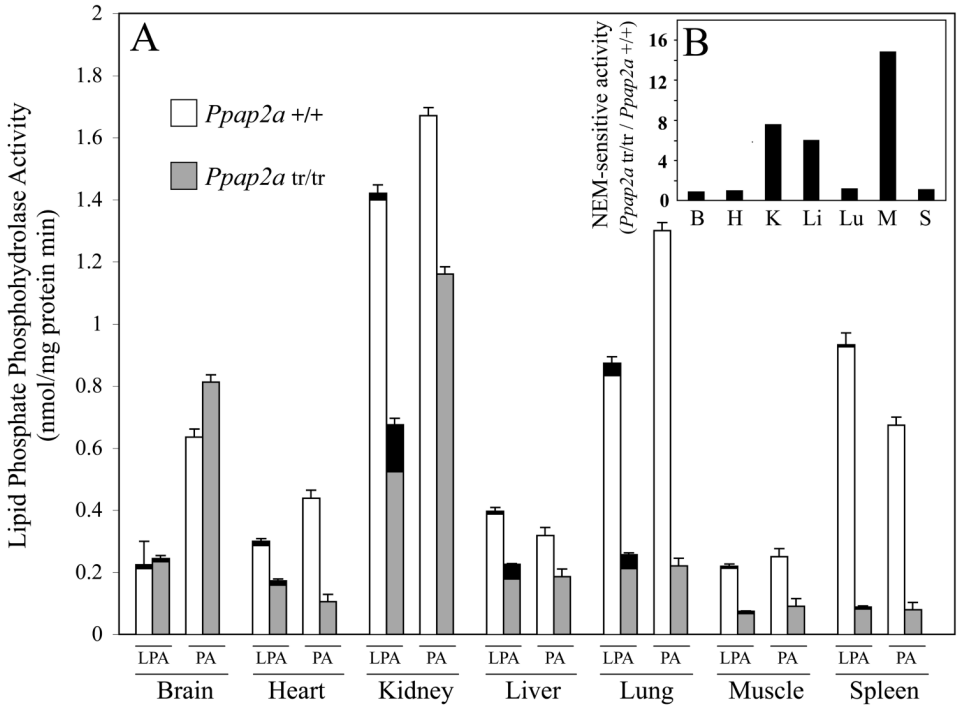

FIGURE 3. Lipid phosphate phosphohydrolase activity of selected organs of *Ppap2a*$^{tr/tr}$ and *Ppap2a*$^{+/+}$ mice

The lipid phosphate phosphohydrolase activity of *Ppap2a*$^{+/+}$ and *Ppap2a*$^{tr/tr}$ mice was measured as the ability of organ homogenates to release [^{32}P]H_3PO_4 from ^{32}P-labeled LPA or PA in a Triton X-100 mixed micelles assay. Main graph (A) shows the lipid phosphate phosphohydrolase activity of *Ppap2a*$^{+/+}$ (white bars) and *Ppap2a*$^{tr/tr}$ (gray bars) mice using either LPA or PA as substrates as indicated in the figure. In the case of LPA, activity was also measured under conditions that abolish the NEM-sensitive, Mg^{2+}-dependent component of the total activity. This is shown as composite LPA bars that represent the total activity as the full height of the bar and the NEM-insensitive, Mg^{2+}-independent activity as the height of the bottom part. Their difference, *i.e.* the NEM-sensitive, Mg^{2+}-dependent portion, is represented by the blackened parts of the bars. Data were obtained from two sets of three animals (three *Ppap2a*$^{+/+}$ and three *Ppap2a*$^{tr/tr}$). Activity is expressed as nmole of [^{32}P]H_3PO_4 released per mg of protein in one minute. Values represent the average ± S.D. for each genotype (n=3). In B, the NEM-sensitive, Mg^{2+}-dependent activity observed in organs of *Ppap2a*$^{tr/tr}$ animals is expressed in relation to the activities observed in the corresponding organs of *Ppap2a*$^{+/+}$ animals, *i.e.* the *Ppap2a*$^{tr/tr}$/*Ppap2a*$^{+/+}$ ratio of NEM-sensitive, Mg^{2+}-dependent activities. For clarity, organs are identified in this case with the initial letter or letters of the their names (“B”: Brain, “H”: Heart, etc).

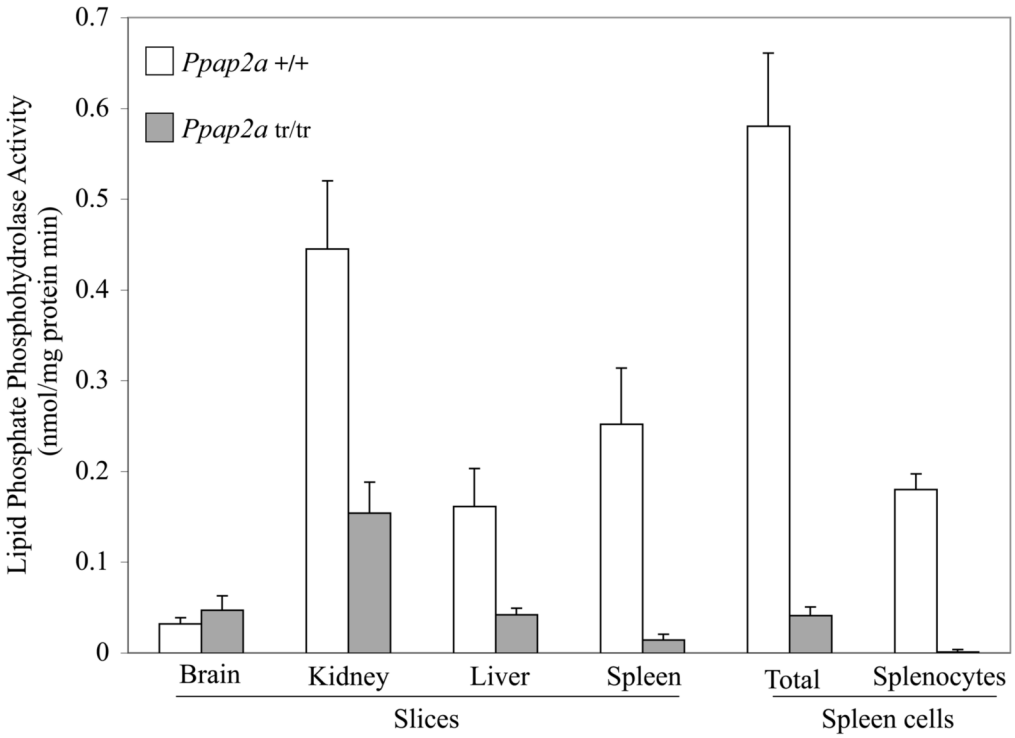

FIGURE 4. Lipid phosphate phosphohydrolase activity of intact cells and tissues from *Ppap2a*$^{tr/tr}$ and *Ppap2a*$^{+/+}$ mice

The lipid phosphate phosphohydrolase activity of small tissue slices and spleen cells from *Ppap2a*$^{+/+}$ and *Ppap2a*$^{tr/tr}$ mice was measured as their ability to release [^{32}P]H_3PO_4 from [^{32}P]LPA. Slices and cells were incubated in a physiological solution containing [^{32}P]LPA for a similar period of time for each tissue or cell type. The leftmost group of bars (indicated as "slices" in the figure) show the phosphohydrolase activity of tissue slices prepared from *Ppap2a*$^{+/+}$ (white bars) or *Ppap2a*$^{tr/tr}$ (gray bars) mice organs. The group of bars on the right indicated as "Spleen cells" in the figure show the phosphohydrolase activity of spleen cells obtained by mechanical disruption of spleens from *Ppap2a*$^{+/+}$ (white bars) or *Ppap2a*$^{tr/tr}$ (gray bars) mice. Bars labeled as "Total" represent the activity of a crude preparation of cells, *i.e.* all the cells that were obtained. "Splenocytes" represents the activity of cell population constituted mostly by lymphocytes that is obtained by removing the red blood cells from a crude preparation by osmotic lysis. Values represent the average ± S.D of four measurements obtained from tissues of two animals and are expressed as nmole of ^{32}P[H_3 PO_4] released per mg of protein in one minute.

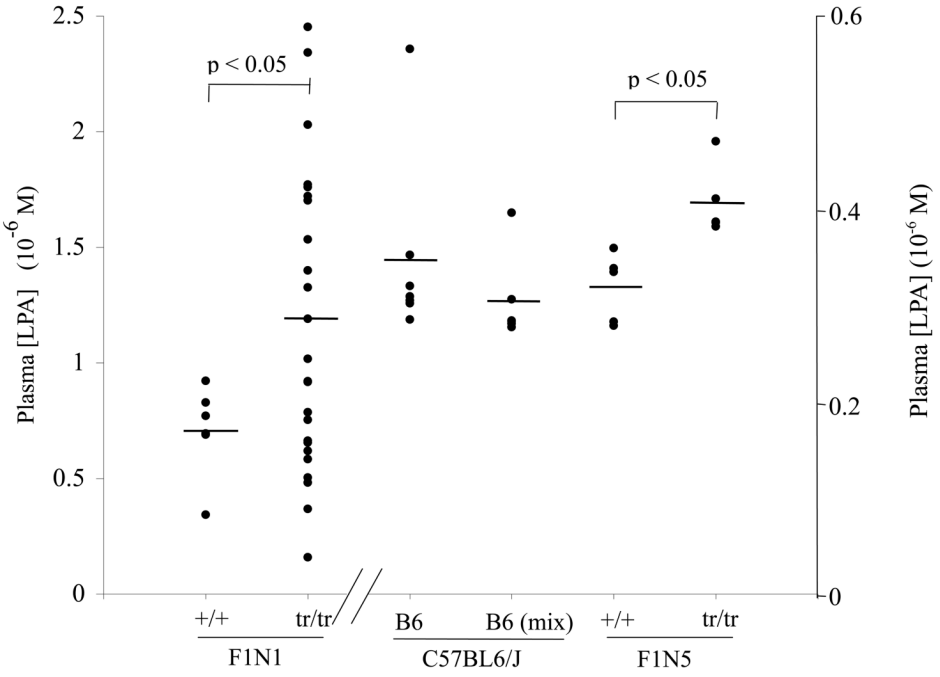

FIGURE 5. Plasma levels of LPA in *Ppap2a*$^{tr/tr}$ and *Ppap2a*$^{+/+}$ mice

The levels of plasma LPA in *Ppap2a*$^{tr/tr}$, *Ppap2a*$^{+/+}$ and C57BL/6j mice were measured by liquid chromatography-mass spectrometry. Each dot represents a single measurement from an individual animal, horizontal bars represent the average. Data for *Ppap2a*$^{tr/tr}$ and *Ppap2a*$^{+/+}$ animals were either F1N1 or F1N5 generations. The biologic and inter-assay variability was assessed in a homogenous C57BL/6j mouse population (4.5 month old females). Values for these animals, depicted as "B6", were 0.35 ± 0.098 μM (n =7). To assess intra-assay variability, portions of the same plasma samples were mixed and assayed repeatedly ("B6mix"). Values in this case were 0.30 ± 0.046 μM (n = 6). Values for F1N1 and F1N5 *Ppap2a*$^{tr/tr}$ mice (n = 5 and n=25 respectively) were significantly higher ($p < 0.05$, Student's *t* test) than those for F1N1 and F1N5 *Ppap2a*$^{+/+}$ mice (n = 5 and n=6 respectively) as indicated in the figure. (Note the split x axis and the magnified y axis (on right), which applies to C57BL/6j and F1N5 animals.)

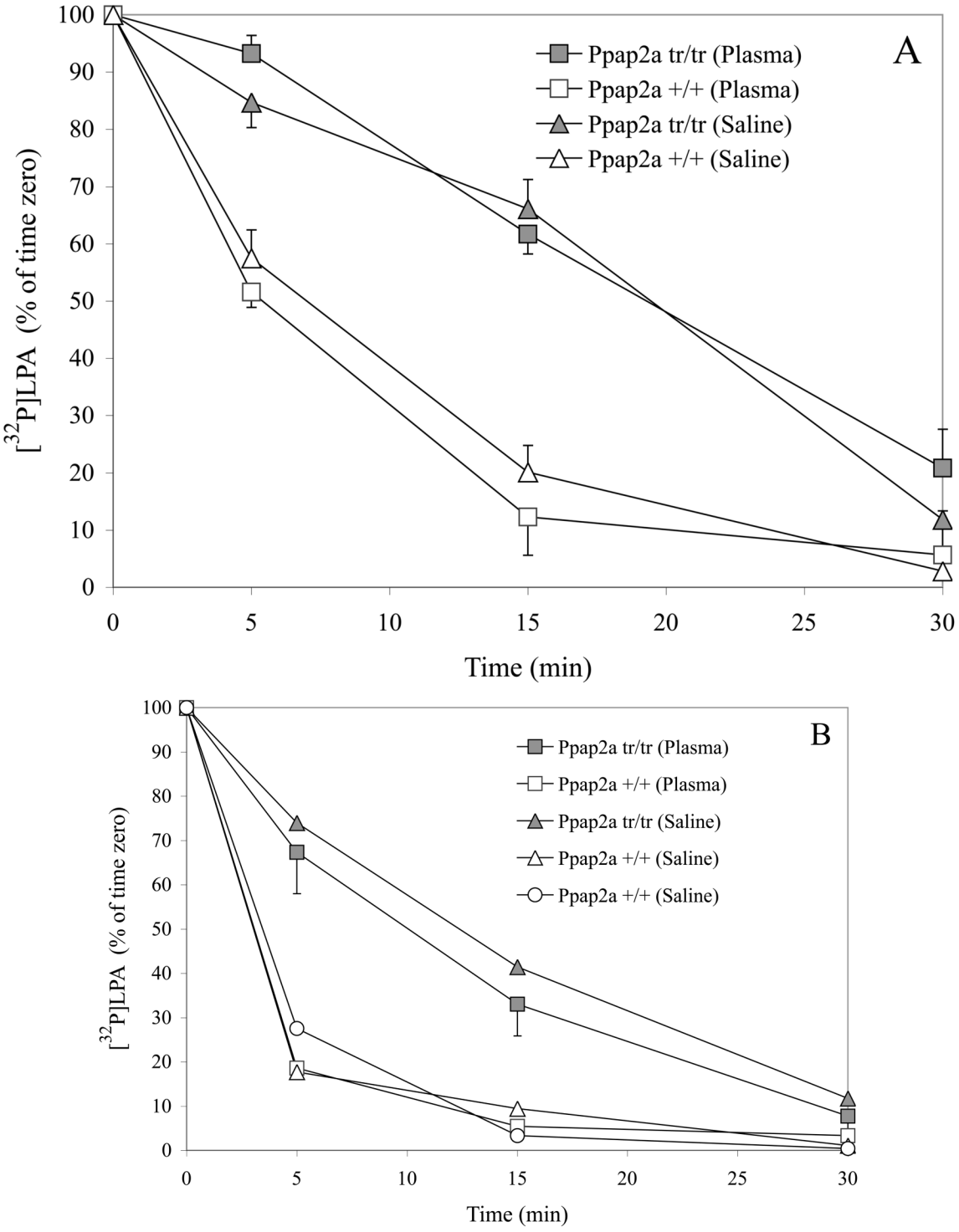

FIGURE 6. ***Ex vivo*** **and** ***in vivo*** **clearance of LPA in** ***Ppap2a*** $^{tr/tr}$ **and** ***Ppap2a*** $^{+/+}$ **mice**

The clearance of LPA was measured by observing the disappearance of [^{32}P]LPA in plasma obtained from blood samples that had been supplemented with tracer amounts [^{32}P]LPA *ex vivo* or *in vivo*. For *ex vivo* experiments, blood samples anticoagulated with EDTA were supplemented with [^{32}P]LPA and incubated for 0, 5, 15 and 30 min at 37°C. Addition of [^{32}P]LPA was accomplished by adding a small amount (5% of the volume of blood) of either

[^{32}P]LPA-containing plasma from another animal of the same genotype or a solution consisting of 0.9 % NaCl, 0.1% FAF-BSA and [^{32}P]LPA. *In vivo* experiments were carried out by injecting mice through the tail vein with 150 μl of either [^{32}P]LPA-containing plasma from another animal of the same genotype or a solution consisting of sterile 0.9 % NaCl, 0.1% FAF-BSA and [^{32}P]LPA. After injection, a series blood samples (~ 50–100 μl) were obtained by retro-orbital bleeding. For practical reasons, the first sample could not be obtained earlier than 2–3 min after injections. This first blood sample was considered to be the "time zero" sample and therefore subsequent samples were taken 5, 15 and 30 min after the moment the first sample was obtained (rather than after the moment of injection). In both cases, *ex vivo* and *in vivo*, plasma was immediately obtained from each timed blood sample by centrifugation and then extracted with 1-butanol under acidic conditions. Butanol extracts were then analyzed by TLC. The amount of [^{32}P]LPA present in each sample was measured by scraping off the [^{32}P]LPA bands from the developed TLC plates and determining their ^{32}P content by liquid scintillation spectrometry. A and B show the results of the *ex vivo* and *in vivo* experiments respectively by expressing the observed amounts [^{32}P]LPA as a percentage of the "time zero" value. In A, the disappearance of [^{32}P]LPA *ex vivo* in blood samples from *Ppap2a*$^{+/+}$ mice (white symbols) and *Ppap2a*$^{tr/tr}$ mice (gray symbols) is shown. Addition of [^{32}P]LPA was carried out as described above by adding plasma (square symbols or "Plasma" in figure) or saline solution (triangular symbols or "Saline" in figure). Each value corresponds to the average ± S.D. of three measurements obtained in blood samples from three different animals. Values for plasma and saline were obtained in blood from the same animals. Plasma used for additions was a combined plasma preparation from two animals. B shows the *in vivo* experiments in which the clearance of [^{32}P]LPA in the bloodstream of live *Ppap2a*$^{+/+}$ (white symbols) and *Ppap2a*$^{tr/tr}$ (gray symbols) mice was measured. Administration of [^{32}P]LPA was carried out as described above by injecting plasma (square symbols or "Plasma" in figure) or saline solution (triangular and circular symbols or "Saline" in figure). Values for *Ppap2a*$^{tr/tr}$ mice injected with saline (gray squares) are the average ± S.D. of three measurements obtained in three different animals. Values for *Ppap2a*$^{tr/tr}$ mice injected with saline (gray triangles) are single determinations. Values for *Ppap2a*$^{+/+}$ mice are single determinations carried out twice with saline (white circles and triangles) and once with plasma (white squares). Because the volume of the blood samples obtained in the *in vivo* experiments were in general not equal, the observed content of [^{32}P] LPA of each sample was corrected by dividing this value by the volume of the "time zero" blood sample. Each injection of plasma was carried out with plasma obtained from a different animal of the same genotype.